PHYSICAL REVIEW D VOLUME 24, NUMBER 5 1 SEPTEMBER 1981

Study of b couplings in the standard weak doublet model and in models without a t quark

V. Barger
Physics Department, University of Wisconsin—Madison, Madison, Wisconsin 53706

W. Y. Keung
Physics Department, Brookhaven National Laboratory, Upton, New York 11973

R. J. N. Phillips
Rutherford and Appleton Laboratories, Chilton, Didcot, Oxon, England
(Received 17 April 1981)

In the context of five-quark models without a t quark, both left-handed b-singlet and right-handed b-doublet options are of interest. We explore the implications of these models, contrasting their predictions with those of the standard six-quark model. In B-meson decays, the singlet model predicts neutral-current modes at a significant level, whereas the $(c,b)_R$ model more closely resembles the standard model. The soft and hard components of the single-lepton energy spectrum can both be used to discriminate between the three classes of models. In neutrino interactions the most promising mechanism is b production from c quarks, which we study in the gluon-fusion and intrinsic-charm models. The b cross section is much larger for the $(c,b)_R$ model. Rates for multilepton final states that might be realized from decays of b and its associated charm spectator are discussed.

I. INTRODUCTION

The nonappearance of t quarks in experimental searches through the mass range up to 19 GeV has sustained interest[1-4] in five-quark models. In the standard SU(2)× U(1) electroweak framework, the simplest such phenomenological model[1-2] adjoins a left-handed singlet b' to the usual $(u, d')_L$, $(c, s')_L$ doublets, where d', s', b' denote orthonormal linear combinations of d, s, b quarks. This leads to large neutral-current (NC) modes for b decay that border on dilepton decay limits.[5] If the model is enlarged[6] by adding a right-handed doublet $(c, b)_R$, the NC modes are greatly reduced.

In the present paper we examine the further experimental implications of these phenomenological five-quark models and contrast their predictions with those of the standard left-handed six-quark model. Section II describes the parameters and known constraints of the models.

Section III discusses the implications for $B_u(b\bar{u})$ and $B_d(b\bar{d})$ meson decays, namely branching fractions, lifetimes, and decay lepton spectra. The singlet model predicts neutral-current modes at a significant level, whereas the $(c, b)_R$ model more closely resembles the standard model. The soft component of the single-lepton spectrum, which comes from $b \to c \to s l \nu$ cascade decays, can be used to determine the fraction of $b \to c$ primary transitions; this fraction is not highly constrained in the standard model but is closely prescribed in both five-quark models. We examine the sensitivity of the soft lepton spectrum component to the $c \to D$ fragmentation function. The hard component of the single-lepton spectrum can be used to discriminate between $V \pm A$ b couplings; the shape near the end point contains additional information about $b \to u$ or $b \to s$ transitions. We illustrate the complete spectrum shape for all three models.

Section IV addresses b production by neutrinos and antineutrinos. The cross sections for b production by neutrinos are much larger for the $(c, b)_R$ model. The most promising mechanism is b production from c quarks, which we study in the gluon-fusion and intrinsic-charm models. Rates for multilepton final states that might be realized from decays of b and its associated charm spectator are discussed. The fact that the favored $\nu \to \mu c\bar{b}$ and $\bar{\nu} \to \bar{\mu} \bar{c} b$ production mechanisms give final states with two charmed particles should help in identifying these processes experimentally.

Section V discusses expectations for B^0-$\bar{B}^0$ mixing in the various models.

II. STRUCTURE OF FIVE-QUARK MODELS

A. Standard model

The standard six-quark model[7] is based upon three left-handed doublets

$$\begin{pmatrix} u \\ d' \end{pmatrix}_L, \quad \begin{pmatrix} c \\ s' \end{pmatrix}_L, \quad \begin{pmatrix} t \\ b' \end{pmatrix}_L, \tag{1}$$

where d', s', b' are orthogonal mixtures of d, s, b quarks. These can be parametrized by the Kobayashi-Maskawa (KM) matrix[7]

$$\begin{pmatrix} d' \\ s' \\ b' \end{pmatrix}_L = \begin{pmatrix} c_1 & s_1c_3 & s_1s_3 \\ -s_1c_2 & c_1c_2c_3 + s_2s_3e^{i\delta} & c_1c_2s_3 - s_2c_3e^{i\delta} \\ -s_1s_2 & c_1s_2c_3 - c_2s_3e^{i\delta} & c_1s_2s_3 + c_2c_3e^{i\delta} \end{pmatrix} \begin{pmatrix} d \\ s \\ b \end{pmatrix}_L \tag{2}$$

in terms of three mixing angles θ_i ($c_i = \cos\theta_i$, $s_i = \sin\theta_i$) and a CP-violating phase δ. With suitable phase conventions for the quark fields, these angles can be restricted to the quadrants $0 \leq \theta_i \leq \pi/2$, $-\pi \leq \delta \leq \pi$. All right-handed quarks are singlets.

The analysis of nuclear and hyperon decays sets the limits[8]

$$s_1^2 = 0.052 \pm 0.005, \quad s_3^2 = 0.08^{+0.13}_{-0.08} \tag{3}$$

and studies of the K_L-K_S mass difference and CP violation lead to bounds[9,10] on the admissible regions of θ_2 and δ; in particular, $0.03 \leq s_2 \leq 0.7$. There are essentially two connected corridors in the space of mixing parameters, called solutions I and II in Ref. 9, characterized by having δ in the first and second quadrants, respectively. Figure 1 shows the corresponding ranges of predictions for $|U_{bu}|$, $|U_{bc}|$, the moduli of the KM matrix elements for $b \to u$, $b \to c$ couplings. Some possible ways to further constrain the KM matrix elements are discussed in Ref. 11.

For the branching fractions and decay spectra discussed in Sec. III, only the ratio of couplings $|b \to u|/|b \to c|$ is significant. We therefore take just two extreme examples of mixing in this model (based on solution I of Ref. 1) that illustrate the allowed range for this ratio, from very small values up to 1:

(i) $s_2 = 0.24$, $s_3 = 0.02$, $\delta = 0.07$,
$|b \to u|/|b \to c| = 0.02$, $|b \to c| = 0.22$;

(ii) $s_2 = 0.6$, $s_3 = 0.5$, $\delta = 0.001$,
$|b \to u|/|b \to c| = 1.0$, $|b \to c| = 0.12$.

We note in passing a third case of later interest (based on solution II of Ref. 9) which corresponds to near maximal $|b \to c|$ coupling strength:

(iii) $s_2 = 0.11$, $s_3 = 0.42$, $\delta = \pi - 0.01$,
$|b \to u|/|b \to c| = 0.2$, $|b \to c| = 0.5$.

We shall return to this case in Sec. IV in our considerations of neutrino production of b from c.

B. Left-handed-singlet model

The simplest phenomenological model[1,2] without a t quark retains the first two doublets above and replaces the third by a left-handed singlet

$$\begin{pmatrix} u \\ d' \end{pmatrix}_L, \quad \begin{pmatrix} c \\ s' \end{pmatrix}_L, \quad (b')_L, \tag{4}$$

where d', s', b' are again defined by the KM mixing matrix Eq. (2). The singlet b' cannot contain substantial admixtures of d and s quarks simultaneously, since this would imply $s \to d$ neutral currents that would give unacceptable corrections to the K_L-K_S mass difference and must be very strongly suppressed. To explain the large kaon multiplicity observed in B decays,[5] b' must then be essentially just a b-s admixture, implying $\theta_2 \simeq 0$ so that δ becomes irrelevant and the mixing is described by only two parameters, θ_1 and θ_3:

$$\begin{pmatrix} d' \\ s' \\ b' \end{pmatrix}_L = \begin{pmatrix} c_1 & s_1c_3 & s_1s_3 \\ -s_1 & c_1c_3 & c_1s_3 \\ 0 & -s_3 & c_3 \end{pmatrix} \begin{pmatrix} d \\ s \\ b \end{pmatrix}_L . \tag{5}$$

This corresponds to solution C of Ref. 1; Refs. 3–4 have examined the full allowed region of very small θ_2, but the essential physics is contained in our approximation $\theta_2 = 0$. The limits of Eq. (3) still apply. With the mixing matrix of Eq. (5), CP violation must have another origin, such as the Higgs sector.

In this model the effective Lagrangian for b-changing interactions is

$$\begin{aligned} \mathcal{L}_{\text{eff}} = &-\frac{4G_F}{\sqrt{2}} s_3[s_1(\bar{u}b)_L + c_1(\bar{c}b)_L][(\bar{l}\nu)_L + c_1(\bar{d}u)_L + s_1c_3(\bar{s}u)_L - s_1(\bar{d}c)_L + c_1c_3(\bar{s}c)_L] \\ &+\frac{2G_F}{\sqrt{2}} s_3c_3(\bar{s}b)_L\{(\bar{\nu}\nu)_L - (1-2x_W)(\bar{l}l)_L + 2x_W(\bar{l}l)_R + (1-\tfrac{4}{3}x_W[(\bar{u}u)_L + (\bar{c}c)_L] - \tfrac{4}{3}x_W[(\bar{u}u)_R + (\bar{c}c)_R] \\ &- (1-\tfrac{2}{3}x_W)(\bar{d}d)_L - (c_3^2 - \tfrac{2}{3}x_W)(\bar{s}s)_L + \tfrac{2}{3}x_W[(\bar{d}d)_R + (\bar{s}s)_R]\} + \text{H.c.}, \end{aligned} \tag{6}$$

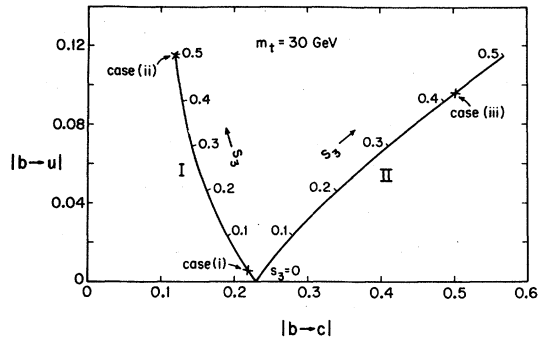

FIG. 1. Predictions of standard-model solutions I and II of Ref. 9 for $b \to u$ and $b \to c$ coupling strengths.

where $(\bar{\alpha}\beta)_L = \bar{\alpha}_L \gamma_\mu \beta_L$, $(\bar{\alpha}\beta)_R = \bar{\alpha}_R \gamma_\mu \beta_R$, and $x_W = \sin^2\theta_W \simeq 0.23$. The dominant charged-current (CC) decay coupling is $b \to c$,

$$|b \to u|/|b \to c| = (s_1 s_3)/(c_1 s_3) = 0.23\,, \tag{7a}$$

and the neutral-current $b \to s$ coupling is comparable to $b \to c$,

$$|b \to s|/|b \to c| = (s_3 c_3)/(c_1 s_3) \simeq 1\,. \tag{7b}$$

The latter leads to the prediction of [1,2] a substantial primary decay branching fraction into lepton pairs

$$B(b \to e^+ e^- X) = B(b \to \mu^+ \mu^- X) \simeq 0.02$$

that is approximately independent of θ_3. This prediction is in some conflict with recent data[5] that set an upper limit of 0.013 for this quantity, with 90% confidence.

There is one corner of mixing-parameter space where our above arguments do not strictly apply. If both the d and s components of b' are very small, it is not necessary that either one of them should be negligible compared to the other; i.e., $b \to d$ and $b \to s$ neutral currents can coexist if both are sufficiently weak. This region is characterized by s_2, s_3 both very small. The mixing matrix then becomes (with $c_2 \simeq c_3 \simeq 1$)

$$\begin{pmatrix} d' \\ s' \\ b' \end{pmatrix} = \begin{pmatrix} c_1 & s_1 & s_1 s_3 \\ -s_1 & c_1 & c_1 s_3 - s_2 e^{i\delta} \\ -s_1 s_2 & c_1 s_2 - s_3 e^{i\delta} & e^{i\delta} \end{pmatrix} \begin{pmatrix} d \\ s \\ b \end{pmatrix}. \tag{8}$$

Suppression of the $d \to s$ neutral current requires[3,4]

$$s_1^2 s_2^2 (c_1^2 s_2^2 - 2 c_1 s_2 s_3 \cos\delta + s_3^2 \cos 2\delta) < 10^{-6}\,.$$

The other NC and CC coupling strengths are

$$|b \to d| = s_1 s_2\,, \quad |b \to u| = s_1 s_3\,,$$
$$|b \to s| = |s_3 - c_1 s_2 e^{i\delta}|\,, \quad |b \to c| = |c_1 s_3 - s_2 e^{i\delta}|\,.$$

Hence the $|b \to u|/|b \to c|$ ratio is not fixed in this solution region, but the sum of the squares of NC and CC couplings are equal:

$$|b \to d|^2 + |b \to s|^2 = |b \to u|^2 + |b \to c|^2\,. \tag{9}$$

This is the analog of Eq. (7b) and has a similar physical consequence, that the NC decay modes are inevitably important. This special class of solutions forms a bridge between solution C and solution U of Ref. 1. For these special solutions with s_2, s_3 small, the b lifetimes are $\tau > 10^{-13}$ s. We do not pursue these special solutions further.

C. Right-handed-doublet model

Tye and Peskin[6] have noted that the NC branching fractions in the five-quark model would be suppressed by the addition of a $(c, b)_R$ current; since the left-handed NC and CC b couplings all contain the factor s_3, a full-strength right-handed current would dominate b decays, giving a substantial strange-quark yield from the $b \to c \to s$ chain.

Let us consider the addition of a general $(c'', b'')_R$ right-handed doublet to the preceding left-handed structure. Here c'' may be any mixture of u, c and b'' may be any mixture of d, s, b. However, u and c cannot coexist substantially in c'' because this would imply $u \to c$ NC couplings and hence strong D^0-$\bar{D}^0$ mixing contrary to experiment.[12] The choice $c'' = u$ is unacceptable because it would give too few kaons in b decay and also would imply a purely vector $\bar{t}u$ neutral current contrary to experiment.[13] Hence $c'' = c$. As to b'', it cannot be dominated by either d or s, since this would spoil the agreement of neutrino-dimuon production with standard LH couplings; nor can b'' contain substantial fractions of d and s simultaneously because of the stringent $d \to s$ NC bound. Thus b'' must be dominantly b with possible small admixtures of either d or s; as a first approximation we put $b'' = b$, so that the additional doublet is simply $(c, b)_R$, as in Ref. 6. The additions to the effective Lagrangian of Eq. (6) are

$$\mathcal{L}_{\rm eff} = -\frac{4G_F}{\sqrt{2}} (\bar{c}b)_R [(\bar{l}\nu)_L + c_1 (\bar{d}u)_L + s_1 c_3 (\bar{s}u)_L - s_1 (\bar{d}c)_L + c_1 c_3 (\bar{s}c)_L] + \frac{2G_F}{\sqrt{2}} s_3 c_3 (\bar{s}b)_L (\bar{c}c)_R + \text{H.c.} \tag{10}$$

Moreover, the $Z^0\,\bar{c}c$ neutral-current coupling due to the $(c, s')_L$ and $(c, b)_R$ doublets is vectorlike.

Since the $(b, c)_R$ doublet dominates, we could now alternatively entertain the hypothesis that the b'_L singlet is a b-d mixture instead. This would correspond to solution U of Ref. 1. For a convenient

parametrization of this case, we can interchange the first two columns in the mixing matrix of Eq. (5) and interchange c_1 and s_1, to obtain

$$\begin{pmatrix} d' \\ s' \\ b' \end{pmatrix}_L = \begin{pmatrix} c_1c_3 & -s_1 & c_1s_3 \\ s_1c_3 & c_1 & s_1s_3 \\ -s_3 & 0 & c_3 \end{pmatrix} \begin{pmatrix} d \\ s \\ b \end{pmatrix}_L . \quad (11)$$

With this option the left-handed (LH) decay amplitudes are still suppressed by s_3 while the bound[8] on the latter becomes stronger: $s_3^2 = 0.004^{+0.007}_{-0.004}$. Inasmuch as the LH contributions are masked by the dominant right-handed (RH) decays, there is little practical value in examining this alternative at present, and we do not pursue it further here.

III. CONSEQUENCES FOR B DECAYS

The decays of b-flavored mesons B_u and B_d can be calculated in a first approximation as the decay of a free b quark with the same mass as the B hadron. The heavy mass scale renders gluon corrections small and the contributions of nonspectator diagrams are not large.[14] The phase space for different quark channels depends somewhat on the assumed quark masses; for our illustrations we use the specific values $m_b = 5.2$, $m_c = 1.87$, $m_s = 0.5$, $m_u = m_d = 0.3$, and the phase-space formulas of Ref. 1. It should be clearly understood that our results for branching fractions, lifetimes, and lepton spectra are intended to be illustrative rather than definitive, since they depend on model assumptions such as mass inputs, neglect of quantum-chromodynamics (QCD) corrections, and neglect of nonspectator diagrams.

In the standard six-quark model, we illustrate the range of possibilities by cases (i) and (ii) described in Sec. II. In the left-handed singlet model, s_1 is fixed and the parameter s_3 affects only the lifetime; all branching fractions are essentially parameter independent. In the right-handed-doublet model we fix s_3 at its central value $s_3 = (0.08)^{1/2}$, with the choice of $b \to c$ dominance in the left-handed sector.

A. Branching fractions

Table I lists the branching fractions of different modes at the quark and lepton spectator-diagram level.[15] The charged-current $b \to c$, $b \to u$ and neutral-current $b \to s$ channels are grouped separately For $b \to sc\bar{c}$ and $b \to su\bar{u}$ decays there are actually contributions from both NC and CC matrix elements; we have ignored their interference, which is permissible since either one matrix element or the other is very small in each case.

Table II gives inclusive branching fractions and multiplicities, derived from the previous table:

TABLE I. b branching fractions in percent.

Channel	Standard model (i)	Standard model (ii)	LH-singlet model	RH-doublet model
$ce\bar{\nu}$	18.8	5.8	8.7	17.4
$c\mu\bar{\nu}$	18.7	5.8	8.6	17.3
$c\tau\bar{\nu}$	4.0	1.3	1.9	3.7
$c\bar{u}d$	48.8	15.2	22.5	45.3
$c\bar{u}s$	2.5	0.6	1.1	2.1
$c\bar{c}s$	6.6	2.2	3.0	6.0
$c\bar{c}d$	0.4	0.1	0.2	0.4
$ue\bar{\nu}$	0.02	11.1	1.2	0.2
$u\mu\bar{\nu}$	0.02	11.1	1.2	0.2
$u\tau\bar{\nu}$	0.01	4.6	0.5	0.1
$u\bar{u}d$	0.05	29.9	3.2	0.4
$u\bar{u}s$	0.002	1.2	0.2	0.02
$u\bar{c}s$	0.02	10.8	1.1	0.1
$u\bar{c}d$	0.001	0.4	0.1	0.01
$s\nu\bar{\nu}$			14.9	2.1
$se\bar{e}$			2.5	0.4
$s\mu\bar{\mu}$			2.5	0.4
$s\tau\bar{\tau}$			0.2	0.02
$su\bar{u}$			8.1	1.1
$sd\bar{d}$			10.4	1.5
$ss\bar{s}$			7.8	1.1
$sc\bar{c}$			0.4	0.1

the subscript PR denotes primary, as distinct from secondary c- or τ-decay contributions.

The most significant property of the LH-singlet model is the strong contribution of $b \to s$ NC decays, observable in various ways[1,2]: (i) a prompt e^+e^- or $\mu^+\mu^-$ signal at 2%, as previously noted; (ii) a large and energetic prompt strange-quark yield, not due to charm decays; (iii) a large two-neutrino mode, with missing energy but no visible leptons.

The RH-doublet model does not differ strongly in any branching fractions from the allowed range of standard-model predictions. Its distinguishing

TABLE II. Inclusive b branching fractions in percent, and multiplicities.

Quantity	Standard model (i)	Standard model (ii)	LH-singlet model	RH-doublet model
$B(b \to cX)_{CC}$	99.9	31	46	92
$B(b \to uX)_{CC}$	0.1	69	7	1.0
$B(b \to sX)_{NC}$			47	7
$B(b \to e^{\pm}X)_{PR}$	19	17	15	18
$\langle N(s+\bar{s}) \rangle$	1.2	0.6	1.2	1.2
$\langle N(s+\bar{s}) \rangle_{PR}$	0.1	0.1	0.7	0.2
$\langle N(c+\bar{c}) \rangle$	1.1	0.4	0.5	1.0

feature is its inflexibility; it predicts a very small fraction of $b \to u$ or $b \to s$ decays of LH-b-singlet origin.

The semileptonic branching fraction for primary electrons is about 18% in the standard or RH-doublet model, whereas the LH-singlet model gives 15%. The significance of the discrepancies with the experimental value[5] $13 \pm 3(\pm 3)\%$ for electrons ($9.4 \pm 3.6\%$ for muons) is unclear, due to possible theoretical enhancement of hadronic modes.

The relative strength of $b \to c$ decay modes relative to $b \to u$ or $b \to s$ modes depends somewhat on the assumed mass of the c quark that affects the phase-space integrals. We have used $m_c = 1.87$ GeV, for which $\Gamma(b \to c)/\Gamma(b \to u) = 0.40 |b \to c|^2 / |b \to u|^2$; had we taken $m_c = 1.70$ or 1.50 GeV instead, the principal $b \to c$ modes would be enhanced by factors 1.14 and 1.4, respectively.

B. Lifetimes

The b lifetime is sensitive to the b mass, scaling approximately with m_b^{-5}. The values below are all calculated for $m_b = 5.2$ GeV.

The standard model admits the range of mean lifetimes[16] for $m_B = 5.2$ GeV,

$$0.8 \times 10^{-14} \lesssim \tau(\text{standard}) \lesssim 1.4 \times 10^{-13} \text{ s}. \quad (12)$$

Figure 2 shows the lifetimes for solutions I and II, plotted versus the $b \to c$ matrix element for varying t-quark mass m_t, that enters in the KM angle analysis of Ref. 9. These results are based on the mass values described above and include (for this calculation only) QCD corrections as in Ref. 16.

In the LH-singlet model the lifetime is proportional to s_3^{-2}, to a good approximation. With the masses assumed here we find in the spectator model

$$\tau(\text{LH singlet}) \simeq 2.2 \times (0.08/s_3^2) \times 10^{-14} \text{ s}. \quad (13)$$

In the RH-doublet model the lifetime is essentially fixed for given m_b. With $m_B = 5.2$ GeV the spectator-decay result is

$$\tau(\text{RH doublet}) \simeq 3.1 \times 10^{-15} \text{ s}. \quad (14)$$

For the standard and LH-singlet cases, these lifetimes should lead to detectable decay lengths in nuclear emulsions. The RH-doublet lifetime, however, seems on the edge of resolvability (e.g., with a typical boost factor $\gamma = 10$ the mean decay length would be 9 microns).

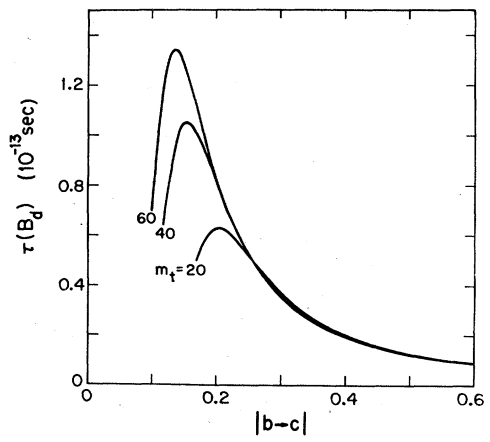

FIG. 2. Standard-model lifetime predictions for solutions I and II vs $|b \to c|$.

C. Decay lepton spectrum

In all models the hard component of the lepton spectrum from b decay comes from the primary $b \to c(u)l\nu$ transitions. Of these, the $b \to ul\nu$ contributions have the higher end point, while the $b \to cl\nu$ contributions may be recognized both by their lower end point and by the softer secondary $c \to sl\nu$ component that they imply.[17,18]

The difference between the LH $b \to c$ couplings (standard and LH-singlet models) and RH $b \to c$ couplings (RH-doublet model) may be seen in the shape of the hard component; LH coupling gives a harder spectrum.

The primary decays may be calculated as free quark transitions, but the secondary decays require additional input about the fragmentation of the c quark to charmed hadrons. In the bulk of our calculations we assume $c \to D$ fragmentation with a fragmentation function $D(z) = 1$ where z is the momentum fraction $z = p_D/p_c$ in the b rest frame. Such a flat fragmentation function is consistent with the neutrino dimuons of charm origin.[19] We calculate D semileptonic decay as an equal superposition[20] of $D \to Kl\nu$ and $D \to K^*l\nu$, which fits the observed spectrum.

The relative strength of $b \to cl\nu$ and $c \to sl\nu$ decays is important for the soft component of the lepton spectrum. Rather than rely on model calculations, we use present experimental indications[5,21] that these branching fractions are approximately equal (when averaged over the B and D charge states produced in e^+e^- collisions).

For cases in which $b \to c$ is dominant, the $(b, c)_R$ model can be distinguished from the $(b, c)_L$ models by the shape of the hard component of the lepton spectrum. Figure 3(a) compares the predicted shapes in the b rest frame. Figure 3(b) shows the present electron data at $\sqrt{s}/2 = 5.27$ GeV with the predictions appropriately boosted and normalized relative to the data. Higher statistics data will be required to differentiate the L, R possibilities.

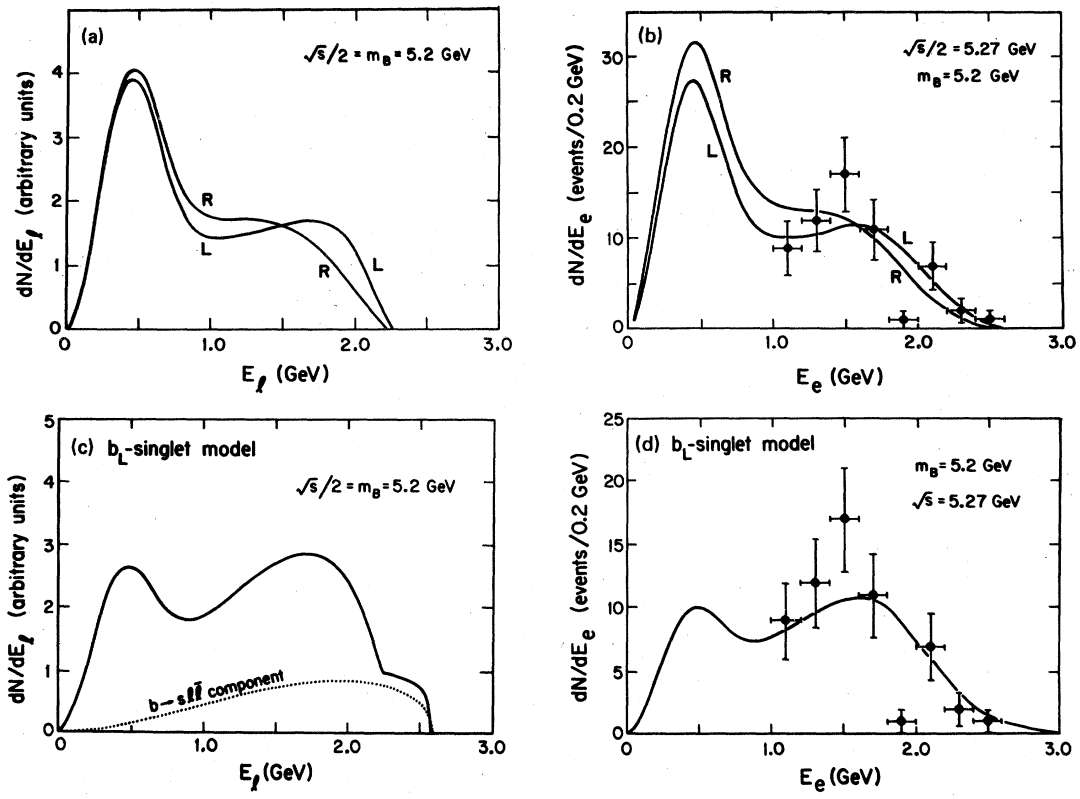

FIG. 3. Single-lepton spectra from B decays (a) at rest for pure $(b,c)_L$ and $(b,c)_R$ models; (b) at $\sqrt{s}=5.27$ GeV for LH and RH models compared with electron spectra from Ref. 5; (c) at rest for b_L-singlet model; (d) at $\sqrt{s}=5.27$ GeV for b_L-singlet model.

The shape of the single-lepton energy distribution depends on the fraction of $b \to c$ primary transitions and can be used to discriminate between models. In the LH-singlet or RH-doublet model, the primary $b \to c$ decay fraction is approximately prescribed, and thereby affords a test of the model. Figures 3(c) and 3(d) show the predictions of the b_L-singlet model, for decays at rest and at $\sqrt{s}/2 = 5.27$ GeV. (Note that in the LH-singlet model each event from the NC mode $b \to s e^+ e^-$ is counted twice in the single-lepton distribution.) Figure 4 shows a range of standard model predictions for B decays at rest corresponding to $|b \to u|/|b \to c|$ ratios 0, 0.3, 0.7, 1, ∞. With K-decay constraints,[9] the $|b \to u|/|b \to c|$ ratio can take any value in the range 0 to 1. The diminution of the soft component and the extension of the end point are associated with an increase in the relative strength of $b \to u$ coupling.[17,18]

Figure 5 illustrates the sensitivity of the soft part of the spectrum to the choice of fragmentation function. The three choices $D(z)=1$, $D(z)=0.16e^{3z}$, $D(z)=\delta(1-z)$ are compared, for the case of $(b,c)_L$ dominance; a hard fragmentation function is advocated in Ref. 22. The charm fragmentation function can be measured directly from $e^+e^- \to \bar{c}c$ events.

D. Dilepton decays

In the standard and RH-doublet models, dilepton modes arise from cascade semileptonic decays $b \to c l \nu$, $c \to s \bar{l} \nu$. In the LH-singlet model, dileptons also arise from neutral-current decays $b \to s l \bar{l}$;

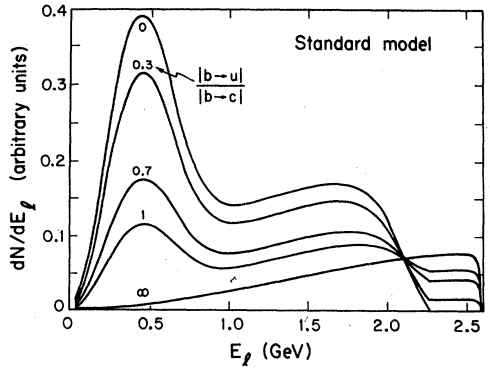

FIG. 4. Single-lepton spectra from b decay at rest in standard model with $|b \to u|/|b \to c| = 0, 0.3, 0.7, 1.0, \infty$.

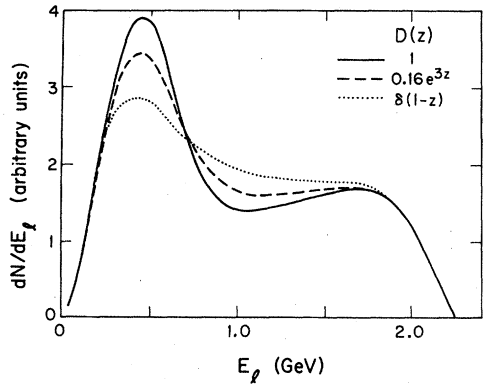

FIG. 5. Single-lepton spectra from b decay at rest for $(b,c)_L$ models with three choices of fragmentation function: $D(z)=1$ (solid curve), $D(z)=0.16e^{3z}$ (dashed curve), $D(z)=\delta(1-z)$ (dotted curve).

these $l\bar{l}$ modes are distinguished by the presence of a fast s quark, no missing neutrino energy, and relatively hard energy distributions for *both* charged leptons. Neutral current modes also include $b \to s\nu\bar{\nu}$ distinguished by large missing energy with no accompanying charged leptons.

The invariant-$l\bar{l}$-mass distributions for the standard, RH-doublet, and LH-singlet models are compared in Fig. 6. The energy distribution of the $l\bar{l}$ pair from b decay at rest is shown in Fig. 7. The distribution in missing $\nu\bar{\nu}$ energy is the same as that of $l\bar{l}$ energy, in all cases.

IV. PRODUCTION OF b QUARKS BY NEUTRINOS

A. General features

Weak couplings of b quarks may be manifested in b production by neutrinos and antineutrinos. In the standard and LH-singlet models the cross sections are rather small, essentially because the couplings to valence u and d quarks are suppressed;

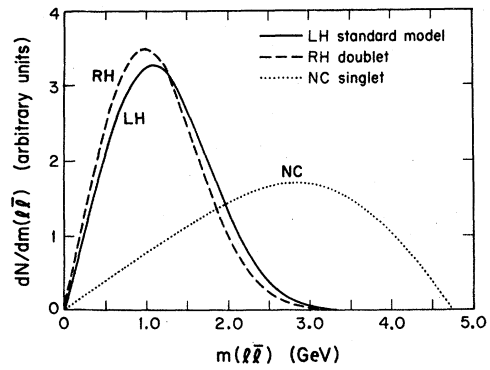

FIG. 6. Invariant-mass distributions of $l\bar{l}$ pairs produced in b decay for the standard model (solid curve), RH-doublet model (dashed curve), and neutral-current component of the LH-singlet model (dotted curve).

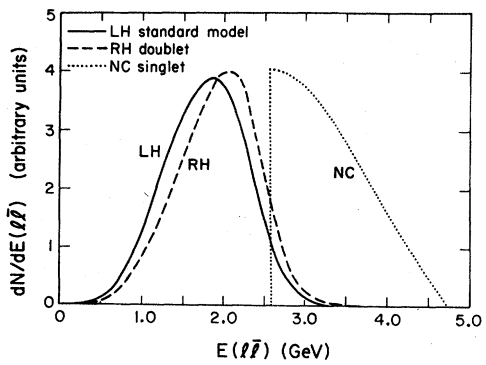

FIG. 7. Distribution of the summed energy of $l\bar{l}$ pairs produced in b decay for the standard model (solid curve), RH-doublet model (dashed curve), and neutral-current component of the LH-singlet model (dotted curve).

there are also threshold suppression effects at presently accessible energies.[23] In the RH-doublet model, however, the $\nu\bar{c} \to \mu\bar{b}$ production mode is enhanced by an order of magnitude. Some b-production events may eventually be detected in emulsions, where the cascade decays would give a distinctive signature.

1. *Quark-parton model*

In b production by neutrinos, the cascade and semileptonic decays of b lead to interesting multilepton signals that could contribute significantly beyond the normal expectations from c and $c\bar{c}$ production.

At the quark level, the contributing processes are

$$\begin{aligned} &\nu\bar{u} \to \mu\bar{b}\,, \quad \bar{\nu}u \to \bar{\mu}b\,, \\ &\nu\bar{c} \to \mu\bar{b}\,, \quad \bar{\nu}c \to \bar{\mu}c\,, \\ &\nu\bar{s} \to \nu\bar{b}\,, \quad \bar{\nu}s \to \bar{\nu}b\,, \\ &\nu s \to \nu b\,, \quad \bar{\nu}\bar{s} \to \bar{\nu}\bar{s}\,, \end{aligned} \tag{15}$$

omitting production from t quarks that is negligible at present energies.[23] The neutral-current modes exist only in the models with a b_L singlet. In the parton-model approximation, the inclusive CC cross sections for b production on a proton target have the forms (in units $G_F^2 M_N E/\pi$)

$$\frac{d\sigma(\nu p \to \mu\bar{b}X)}{dx\,dy} = \epsilon_L^u \bar{u}(x_u)\overline{Y}_u + \epsilon_L^c \bar{c}(x_c)\overline{Y}_c + \epsilon_R^c \bar{c}(x_c)Y_c \tag{16}$$

while the NC cross sections in the LH-singlet model of Eq. (5) are

$$\begin{aligned} &\frac{d\sigma(\nu p \to \nu b X)}{dx\,dy} = \tfrac{1}{4}s_3^2 c_3^2 s(x_s)Y_s\,, \\ &\frac{d\sigma(\nu p \to \nu\bar{b}X)}{dx\,dy} = \tfrac{1}{4}s_3^2 c_3^2 \bar{s}(x_s)\overline{Y}_s\,. \end{aligned} \tag{17}$$

Here $\bar{u}(x)$, etc., denote the quark fractional momentum distributions in the target proton. For antineutrino production, interchange ν with $\bar{\nu}$, μ with $\bar{\mu}$, b with $\bar{b}$, etc., throughout Eqs. (16) and (17). The slow-rescaling[24] variables x_a ($a = u, s, c$) are defined by

$$x_{\tilde{a}} = x + (m_b^2 - m_a^2)/(2M_N\nu)\,, \tag{18}$$

where $x = Q^2/2M_N\nu$ and $\nu = Ey$ as usual. The y-dependent factors are

$$\begin{aligned} Y_a &= 2x_a + 2y(x - x_a)\,, \\ \bar{Y}_a &= 2(x_a - xy)(1 - y)\,. \end{aligned} \tag{19}$$

The couplings are defined by $\epsilon^a_{L,R} = |U_{L,R}(b, a)|^2$ where U is the mixing matrix. We take the hadronic threshold energy to be $W = M_N + m_b$ for production from uncharmed quarks, $W = M_N + m_b + m_c$ for production from charmed quarks.

2. Gluon-fusion model

The distribution of charmed quarks in the nucleon is an important input. The current-gluon-fusion model[25,26] provides a plausible dynamical model for the $c\bar{c}$ sea, which is already known to give a good description of charm production data with muon beams.[27] The gluon-fusion diagram for $\nu g \to \mu\bar{b}c$ is shown in Fig. 8; the differential cross section for this process can be conveniently written for $(b, c)_L$ coupling as

$$d\hat{\sigma}(\nu g \to \mu\bar{b}c) = \frac{\sum |M|_L^2}{8\hat{s}(2\pi)^5} \frac{d\vec{\mu}\, d\vec{b}\, d\vec{c}}{8\mu_0 b_0 c_0} \delta^4(\nu + g - \mu - b - c)\,, \tag{20}$$

with

$$\sum |M|_L^2 = \frac{512\pi G_F^2 \alpha_s \epsilon_L^c}{(1 + Q^2/M_W^2)^2} \left[\frac{(g\cdot\mu - c\cdot\mu)(b\cdot\nu)}{c\cdot g} \left(1 + \frac{c\cdot c}{c\cdot g} - \frac{b\cdot c}{b\cdot g}\right) + \frac{(c\cdot\mu)(c\cdot\nu)}{c\cdot g} + \begin{pmatrix} b \to c,\ \mu \to \nu \\ \text{simultaneously} \end{pmatrix} \right], \tag{21}$$

where $\hat{s}$ is the subprocess invariant energy squared and α_s is the gluon coupling constant. In these formulas the symbols denote the four-momenta of the particles, with the exception that b denotes the momentum of the outgoing $\bar{b}$. For the case of full-strength $(b, c)_R$ coupling, ν and μ are interchanged in Eq. (21) and ϵ_L^c is replaced by 1.

The full cross section on nucleons is obtained by convolution with the gluon distribution:

$$d\sigma(\nu N \to \mu\bar{b}cX) = \int_{\eta_0}^1 d\eta\, G(\eta) d\hat{\sigma}\,, \tag{22}$$

where $\eta = \hat{s}/s$ and $\eta_0 = (4m_c^2 + Q^2)/s$. We shall use the gluon distribution deduced from charm production analyses[27,28] $G(\eta) = 3(1 - \eta)^5/\eta$.

3. Intrinsic-charm model

Motivated by the large observed cross sections for diffractive charm production, it has been suggested that the nucleon contains long-lived "intrinsic" charm components in $qqqc\bar{c}$ Fock states, and a simple model gives the distribution[29,30]

$$\begin{aligned} c(x) = \bar{c}(x) = 600\lambda x^2[&(1 - x)(1 + 10x + x^2) \\ &+ 6x(1 + x)\ln x]\,, \end{aligned} \tag{23}$$

where $\lambda = \int c(x)dx$ is estimated to be of order 0.01.

The intrinsic-charm contribution is expected to be additive to the gluon-fusion charm component, since it has a different dynamical origin. In muoproduction intrinsic charm enters mainly at large Q^2 and is not in conflict[27] with gluon-fusion analyses of existing data[31,32] at low Q^2. However, a stringent limit on λ is provided by recent high-statistics dimuon results from the European Muon Collaboration[33] (EMC) at 250 GeV and large Q^2. The data have been analyzed in terms of $F_2(\text{charm}) = \frac{8}{9} xc(x)$, assuming $c \to D$ fragmentation function $D(z) = 1$ in the laboratory frame. The intrinsic-charm prediction with $\lambda = 0.01$ lies three standard deviations (equivalent to a factor of three in λ) above the data point at $\nu = 130$ GeV, $Q^2 = 70$ GeV^2 and two standard deviations above the data point at $\nu = 190$ GeV, $Q^2 = 70$ GeV^2. Hence the normalization $\lambda = 0.01$ is an extreme upper value; we use this value in our illustrations.

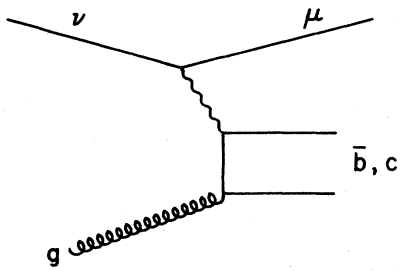

FIG. 8. Diagram of the subprocess $\nu g \to \mu\bar{b}c$.

B. Total cross sections for b production

We calculate contributions from struck u, $\bar{u}$, s, $\bar{s}$ quarks using the parton-model formulas Eqs. (16)–(17) with QCD-corrected parton distributions from the counting-rule solution of Owens and Reya.[34]

We calculate contributions from c, $\bar{c}$ quarks using either the gluon-fusion model (with $m_c = 1.5$ GeV, $\alpha_s = 12\pi/\{23 \ln[(Q^2 + m_{c\bar{b}}^2)/\Lambda^2]\}$, $\Lambda = 0.5$ GeV) or intrinsic charm, with strength $\lambda = 0.01$.

Figure 9 shows the contributions from $\bar{c}$, $\bar{s}$, and s to neutrino production of b, $\bar{b}$ on an isospin-averaged nucleon target, as fractions of the total CC cross section $\sigma(\nu N \to \mu X) = 0.63(E/\text{GeV}) \times 10^{-38}$ cm^2. The $\bar{u} \to \bar{b}$ contribution is shown in Fig. 9(a); Figs. 9(b) and 9(c) show the $\bar{c} \to \bar{b}$ contribution for the gluon model and the intrinsic-charm model separately; Fig. 9(d) displays the neutral-current $s \to b$, $\bar{s} \to \bar{b}$ contributions of the five-quark models.

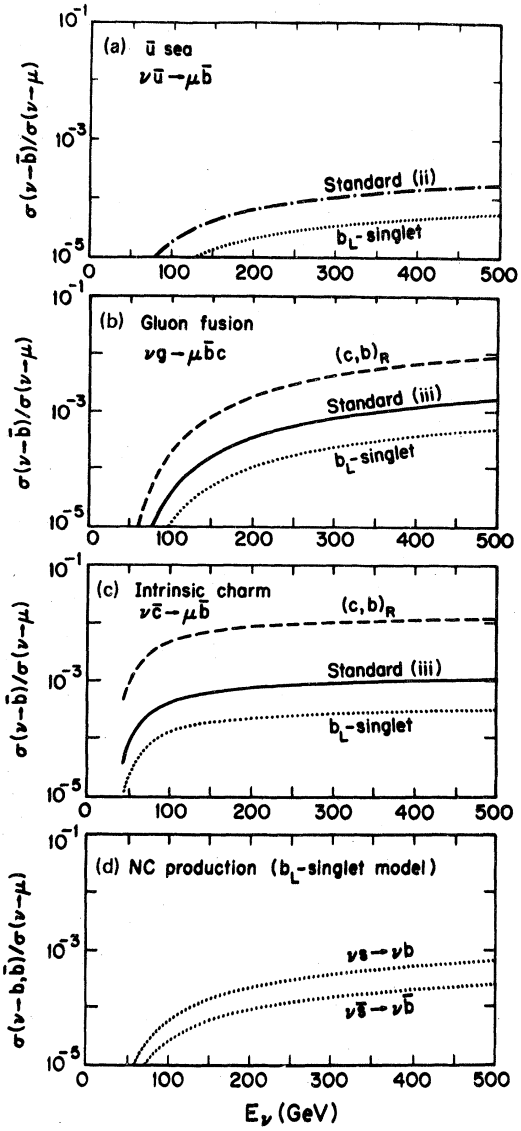

FIG. 9. Neutrino production of b and $\bar{b}$ from an isospin-averaged nucleon target, as a fraction of the total charged-current cross section. (a) $\bar{u} \to \bar{b}$ contribution. (b) $\bar{c} \to \bar{b}$ with gluon-fusion model. (c) $\bar{c} \to \bar{b}$ with intrinsic-charm model with strength $\lambda = 0.01$. (d) neutral-current $s \to b$, $\bar{s} \to \bar{b}$ contributions. Solid curves denote standard model (iii) with near maximal $(c,b)_L$ coupling; dot-dashed curves denote standard model (ii) with maximal $(u,b)_L$ coupling; dotted curves denote the LH-singlet model; dashed curves denote the RH-doublet model $(c,b)_R$, in cases where it differs from the LH-singlet model.

Antineutrino production from the u quarks in an isospin-averaged nucleon is shown in Fig. 10, as a fraction of the total CC cross section $\sigma(\bar{\nu}N \to \bar{\mu}X) = 0.30(E/\text{GeV})10^{-38}$ cm^2. The contributions from c, s, $\bar{s}$ quarks can be read from Fig. 9, by charge-conjugating the participating quarks and leptons and scaling up by the $\nu/\bar{\nu}$ cross-section ratio 2.1.

These results show that for neutrino production the most promising channel is $\bar{c} \to \bar{b}$, especially with an intrinsic-charm component and a $(b,c)_R$ current. We concentrate our attention on these transitions. For antineutrino production the $u \to b$ channel may also be significant, but only if the $(u,b)_L$ coupling is near maximum.

We observe that the most favored $\nu\bar{c} \to \mu\bar{b}$ process will give final states with two charmed particles (from $\bar{b}$ decay and the spectator c) that could be identified in emulsions. This also implies a high kaon multiplicity that could be detected in bubble chambers.

C. Multilepton signals

The primary and cascade decays of b into muons and electrons lead to possibly identifiable multileptons signals. Along with the $\bar{b}$ produced in $\nu\bar{c} \to \mu\bar{b}$, there is an accompanying spectator c quark whose decay can contribute an additional lepton. We discuss the various lepton signals in neutrino scattering below. The corresponding diagrams are shown in Fig. 11 for the neutrino case.

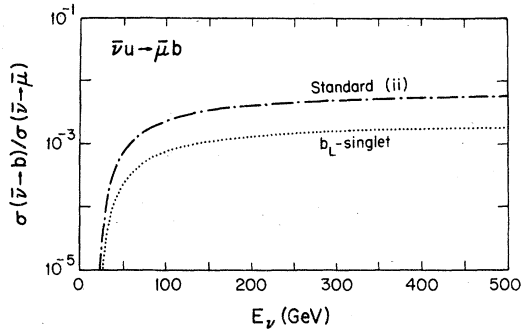

FIG. 10. Antineutrino production $\bar{\nu}u \to \bar{\mu}b$ from u quarks in an isospin-averaged nucleon target, as a fraction of the total charged-current cross section. Labeling of curves follows the notation of Fig. 9.

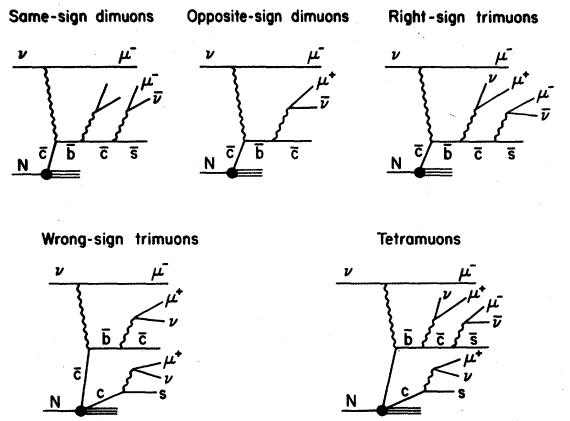

FIG. 11. Diagrams for multilepton states from b production and decay.

1. Wrong-sign single leptons

Wrong-sign single-muon or single-electron events $\nu N \to l^+ X$, $\bar{\nu} N \to l^- X$ could be signatures for new-flavor production by neutral currents. An experimental limit for neutrinos has been given[35]:

$$N(\nu \to \mu^+)/N(\nu \to \mu^-) < 1.6 \times 10^{-4} \quad (90\%\ \text{C.L.}) \quad (24)$$

for $E_\mu > 5.5$ GeV, averaged over the CERN narrow-band beam with $100 < E_{\text{vis}} < 200$ GeV (the spectrum is flat in this energy range). This has been converted into the following upper bound on the neutral-current charm production cross section

$$\sigma(\nu N \to \nu c \bar{c} X)/\sigma(\nu N \to \mu^- X) < 8 \times 10^{-3} \quad (25)$$

for $E \simeq 150$ GeV, after correcting for missing energy in E_{vis}, for the charm semileptonic branching fraction and for the muon-detection efficiency.[35]

Wrong-sign single-lepton processes $\nu N \to l^+ X$ ($\bar{\nu} N \to l^- X$) arise from neutral-current scattering, for example from $\nu c \to \nu c$ with semileptonic decays $c \to s l^+ \nu$. Far above threshold where slow rescaling effects can be ignored, the integrated NC cross section on the c-quark component of the nucleon is

$$\sigma(\nu c \to \nu c) = (G^2 ME/\pi)\left[\tfrac{1}{2}(1 - \tfrac{4}{3}x_W)^2 + \tfrac{1}{6}(a - \tfrac{4}{3}x_W)^2\right] \int_0^1 xc(x)dx, \quad (26)$$

where $a = 0$ in the standard and LH-singlet models, $a = 1$ in the RH-doublet model. We ignore the $\nu \bar{c} \to \nu \bar{c}$ cross section

$$\sigma(\nu \bar{c} \to \nu \bar{c}) = (G^2 ME/\pi)\left[\tfrac{1}{2}(a - \tfrac{4}{3}x_W)^2 + \tfrac{1}{6}(1 - \tfrac{4}{3}x_W)^2\right] \times \int_0^1 x\bar{c}(x)dx \quad (27)$$

since the μ^+ from the spectator c decay would be slow and unlikely to be detected.

The intrinsic-charm component is bigger than the gluon-fusion charm component and gives $\int xc(x)dx = 2\lambda/7$. Equations (25)–(26) then lead to upper bounds on the intrinsic-charm strength[36]

$$\lambda < \begin{cases} 0.05 & (a=0) \\ 0.04 & (a=1) \end{cases} \quad (28)$$

that are conservative, since threshold suppression of charm production is not included in Eq. (26). These bounds are not restrictive, when compared with the value $\lambda \simeq 0.01$ used[29,30] to explain diffractive charm production observations.

Wrong-sign single leptons can also arise from neutral-current b production, $\nu s \to \nu b$, $\nu \bar{s} \to \nu \bar{b}$ with subsequent $b \to c \to s\mu^+\nu$ or $\bar{b} \to \bar{c}\mu^+\nu$. Multiplying the production rates in Fig. 9 by the semileptonic branching fractions of order 0.1, we see that the wrong-sign single-lepton signal from this source would be well below the upper limit Eq. (24). It would therefore be extremely difficult to extract a b signal here, since the backgrounds from $\bar{\nu}$ contamination in the beam and misidentified dimuons are typically[35] much bigger than the upper limit of Eq. (24).

2. Same-sign dileptons

Recent observations[37–39] of a substantial same-sign dimuon signal $\nu N \to \mu^- \mu^- X$ are of interest in connection with possible b production. The rate is at least two order of magnitude above the lowest-order QCD calculations[40] for associated charm production in the hadronic vertex $\nu N \to \mu c \bar{c} X$ with semileptonic $\bar{c} \to \bar{s}\mu\bar{\nu}$ decay.

A signal would be expected from $\nu \bar{c} \to \mu \bar{b}$ production, with $\bar{b} \to \bar{c} \to \bar{s}\mu\bar{\nu}$ decay. Figure 12 shows the predicted rates for the standard left-handed model with maximum coupling $|b \to c| = 0.5$ and for the RH-doublet model with $|b \to c| = 1$; in each case the gluon-fusion and intrinsic-charm (with $\lambda = 0.01$) cross sections are calculated. We assume the produced $\bar{b}$-quark fragments into a B meson of the same momentum.[22] The B decay is treated as in Sec. III C, with 10% charm semileptonic branching fraction, and acceptance cuts $E_\mu > 9$ GeV. The results are compared with data from Ref. 38 ($E_\mu > 10$ GeV cuts) and Ref. 39 ($E_\mu > 9$ GeV cuts).

These results show that the RH-doublet model could explain an interesting fraction of the same-sign dimuon rate if the intrinsic-charm model is invoked. With any of the other models considered here, very little of the same-sign dimuon rate can be accounted for.

With the b-production mechanisms, the predicted antineutrino rate of same-sign dileptons is approximately

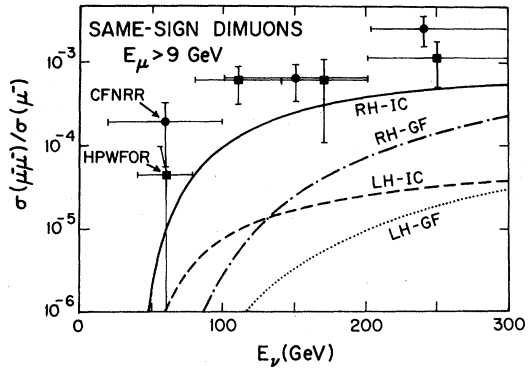

FIG. 12. Predicted same-sign-dimuon rates on an isospin-averaged nucleon target from $\nu\bar{c} \to \mu^- \bar{b}$ production in standard model (iii) with near-maximum allowed $(b,c)_L$ coupling and in the RH-doublet model with full-strength $(b,c)_R$ coupling. The cross sections are based on gluon fusion (GF) and intrinsic charm (IC) with strength $\lambda = 0.01$. The representation is as follows: RH-IC (solid curve), LH-IC (dashed curve), RH-GF (dash-dotted curve), LH-GF (dotted curve). Data are from Refs. 38 and 39.

$$\frac{N(\bar{\nu} \to \mu^+\mu^+)}{N(\bar{\nu} \to \mu^+)} \simeq 2\frac{N(\nu \to \mu^-\mu^-)}{N(\nu \to \mu^-)} . \tag{29}$$

For antineutrinos the process $\nu u \to \mu^+ b$ on the valence u quark gives additional b production; however, even if the $(u,b)_L$ coupling approaches its maximal allowed value 0.1, this contribution is still below the maximum $(c,b)_R$ contribution discussed above.

A possible element neglected above is $\bar{B}^0$-B^0 mixing. If this mixing were strong, up to half the $\bar{b} \to \mu^-$ decays might come from the first rather than the second step of the decay chain. The μ^- spectrum would then be somewhat harder and its acceptance losses smaller. The net $\bar{b} \to \mu^-$ branching fraction would be little changed since both steps have about the same semileptonic branching fraction. Quantitative estimates of mixing effects depend on the ratio of charged to neutral B production and the amount of mixing. As an illustration, we assume a production ratio $B^+ : B^0 = 1:1$ with maximal B^0-$\bar{B}^0$ mixing, in which case one-fourth of the secondary μ^- originate from the first stage of the decay chain. The $N(\mu^-\mu^-)/N(\mu^-)$ ratio is increased at $E = 100$, 200 GeV by factors of about 1.6, 1.3 for the $(c,b)_L$ model and 1.4, 1.2 for the $(c,b)_R$ model, with an $E_\mu > 9$ GeV acceptance cut. Corrections in the rate of this order would not alter our previous conclusions. The predictions of the $\bar{b}$-production models for average values of distributions in $\nu \to \mu^-\mu^-$ at $E = 185$ GeV are tabulated in Table III and compared with the Nishikawa *et al.* data.[39]

3. *Opposite-sign dileptons*

There will also be a contribution from b production to opposite-sign dilepton signals at a rate comparable to the same-sign dilepton rate, with the secondary lepton originating in the first stage of the b-cascade decay (or in the second stage with B^0-$\bar{B}^0$ mixing). This would contribute some secondary leptons at large transverse momentum, which could eventually be helpful in isolating the b signal. The presence of two charmed particles in the final state could also help to identify these events.

4. *Right-sign trileptons*

"Right-sign" trimuon production $\nu N \to \mu^-\mu^-\mu^+ X$, $\bar{\nu} N \to \mu^+\mu^+\mu^- X$ is predicted for $\nu\bar{c} \to \mu\bar{b}$ and $\bar{\nu}c(u) \to \bar{\mu}b$ processes with double semileptonic decay $b \to c\mu\bar{\nu}$, $c \to s\bar{\mu}\nu$. Such trimuons have been observed,[41,42] but are interpreted as due mainly to ordinary charged-current scattering with a low-

TABLE III. Average quantities for $\nu \to \mu^-\mu^-$ for incident energy $E = 185$ GeV. B^0-$\bar{B}^0$ mixing results are based on equal B^+ and B^0 production. Data and definition of quantities are given in Nishikawa *et al.* (Ref. 39).

		No B^0-$\bar{B}^0$ mixing		Maximal B^0-$\bar{B}^0$ mixing	
Quantity	Experiment	$(c,b)_R$	$(c,b)_L$	$(c,b)_R$	$(c,b)_L$
$E_{\rm vis}$ (GeV)	179 ± 19	173	176	168	173
E_h (GeV)	101 ± 14	93	72	82	63
$p_{\mu 2}$ (GeV)	14 ± 2	17	16	20	19
p_{12}^s (GeV)	0.63 ± 0.14	0.83	0.58	1.0	0.82
ϕ (deg)	131 ± 8	140	141	138	138
$x_{\rm vis}$	0.22 ± 0.07	0.24	0.21	0.23	0.21
$y_{\rm vis}$	0.63 ± 0.05	0.64	0.50	0.60	0.47
z_μ	0.17 ± 0.02	0.17	0.20	0.23	0.27
$W_{\rm vis}$	12.7 ± 1.2	12.4	11.3	12.0	10.8

mass hadronic or electromagnetic lepton pair.[42,43] On the basis of the invariant-mass distribution of the slow $\mu^-\mu^+$ pair, an upper limit has been set on the trimuon contribution from b decays,

$$\sigma(\nu \to \mu^-\mu^-\mu^+)/\sigma(\nu \to \mu^-) < 7\times 10^{-6}, \quad (30)$$

for the CERN wide-band beam with $E \geq 30$ GeV and $E_\mu \geq 4.5$ GeV.

For the standard model with maximum allowed $(c,b)_L$ coupling and for the RH-doublet model with full-strength $(c,b)_R$ coupling we calculate corresponding values consistent with the above bound:

$$\sigma(\nu \to \mu^-\mu^-\mu^+)/\sigma(\nu \to \mu^-) = \begin{cases} 0.6\times 10^{-6}, & \text{LH-IC} \\ 7.7\times 10^{-6}, & \text{RH-IC} \end{cases} \quad (31)$$

for intrinsic charm (IC) with $\lambda = 0.01$. The gluon-fusion mechanism gives smaller values. The predicted rates for b-produced trimuons are shown along with the data[41,42] in Fig. 13. These rates are not affected by B^0-$\bar{B}^0$ mixing. The RH-doublet model predicts the strongest signal; the invariant mass of the $\mu^+\mu^-$ pair from cascade b decay (see Fig. 6) provides the cleanest test of this mechanism.

5. *Wrong-sign trileptons*

"Wrong-sign" trimuon production $\nu N \to \mu^-\mu^+\mu^+X$ production is predicted for $\nu\bar{c} \to \mu\bar{b}$ with $\bar{b} \to \bar{c}\mu\nu$ and $c \to s\mu\nu$ decays of the produced $\bar{b}$ and spectator c. A few such events have been reported[42] but are consistent with conventional backgrounds.

The total rate of such events for neutrinos (and correspondingly for antineutrinos) may be read from Fig. 9, multiplying by 0.01 for the product of b and c semileptonic branching fractions. An acceptance-corrected rate is hard to estimate, for the intrinsic-charm model that gives the biggest

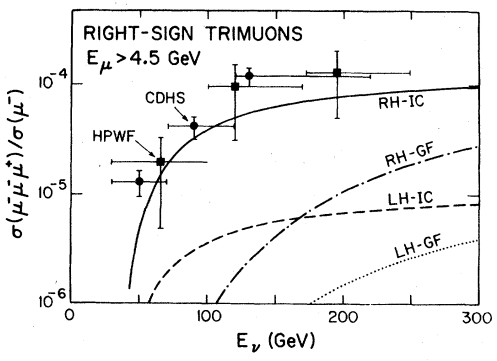

FIG. 13. Predicted right-sign-trimuon rates on an isospin-averaged nucleon target from $\nu\bar{c} \to \mu^-\bar{b}$ production, with $E > 4.5$ GeV acceptance cuts. Curves are labeled as in Fig. 12. Data are from Refs. 41 and 42.

cross sections, since we have no prescription here for the energy of the spectator c quark. Qualitatively these events should be characterized by a rather slow μ^+ from the spectator decays (μ^- for antineutrinos).

6. *Tetraleptons*

Events with four leptons $\nu N \to \mu^-\mu^-\mu^+\mu^+X$ will be produced by $\nu\bar{c} \to \mu\bar{b}$ with semileptonic decays of $\bar{b}$, the cascade $\bar{c}$, and the spectator c. The total rate of such events relative to CC events may be read from Fig. 9, multiplying by 0.001 for the product of three semileptonic branching fractions (and by a further 2.1 for antineutrinos). As in the previous subsection, we are unable to calculate acceptance corrections for the intrinsic-charm model. These events will be characterized by a slow muon from spectator c-decay.

A few such events have been observed.[44] Conventional mechanisms are evaluated in Ref. 45.

7. *Neutral-current ψ and $c\bar{c}$ production*

In the standard and LH-singlet models the $c\bar{c}$ neutral current has the usual couplings $g_L = 1 - \frac{4}{3}x_W$, $g_R = -\frac{4}{3}x_W$ [see, e.g., Eq. (6)]; in the RH-doublet model, however, the coupling is purely vectorlike, $g_L = g_R = 1 - \frac{4}{3}x_W$. The $c\bar{c}$ current can be probed directly by ψ production $\nu N \to \nu\psi X$.

The gluon-fusion model gives a good description[27,46] of elastic ψ production by the electromagnetic current $\mu N \to \mu\psi X$, with the ansatz that ψ states arise from a fixed fraction of bare quark production $\mu N \to \mu c\bar{c}X$ in the narrow invariant-mass interval $2m_c \leq m(c\bar{c}) \leq 2m_D$. Applying this model in the narrow-window approximation to neutrino neutral-current production, we predict that

$$\frac{d\sigma(\nu N \to \nu\psi X)/d\nu\, dQ^2}{d\sigma(\mu N \to \mu\psi X)/d\nu\, dQ^2} = \frac{9G_F^2Q^4}{64\pi^2\alpha^2}(g_L^2 + g_R^2) \quad (32)$$

at each kinematic point (ν, Q^2), for diffractive ψ events (i.e., with little accompanying hadronic energy, typically $E_{\rm had} < 5$ GeV).

For the standard model, the spectrum-averaged rate prediction for diffractive ψ production with $\psi \to \mu^+\mu^-$ decay is[47]

$$N(\nu \to \psi \to \mu^+\mu^-)/N(\nu \to \mu^-) = 2\times 10^{-6} \quad (33)$$

for the CERN 350-GeV wide-band beam. For the RH-doublet model this prediction is increased by a factor 1.7. In the latter model, since the neutral current is vectorlike, the ratio to muoproduction is essentially model independent. Inasmuch as the gluon-fusion model effectively parametrizes the muoproduction data, the predicted neutrino rate is free of model dependence in this case. Some ψ

production has already been observed[48] at the predicted order of magnitude; an accurate measurement could discriminate between the standard and RH-doublet models.

The neutral-current cross section for open $c\bar{c}$ production by neutrinos or antineutrinos is also a direct measure of $g_L^2+g_R^2$ and hence a discriminator of models. In the parton model for the above threshold, we have again Eq. (32) with $c\bar{c}$ written in place of ψ. Muoproduction of charm has been measured through dimuon and trimuon events.[31,32] Neutral-current charm production may be measurable in emulsions; one candidate event has recently been reported.[49]

IV. B^0-$\bar{B}^0$ MIXING

The study of B^0-$\bar{B}^0$ meson mixing could shed light on the structure of b-quark weak interactions.[7,50-52] We concentrate attention here on the $B_d^0(\bar{b}d)$ state.

A. Standard model

Using KM-angle determinations from analyses of K^0-$\bar{K}^0$ mixing, predictions of B^0-$\bar{B}^0$ mixing have been made in Ref. 51. Within each of the two solution classes I and II, the amount of B^0-$\bar{B}^0$ mixing depends on two parameters s_3 and the t-quark mass m_t. Figure 14 illustrates predictions based on Ref. 51 for the time-integrated mixing measure $2\Delta/(1+\Delta^2)$ versus $|b\to c|$ or $|b\to u|/|b\to c|$ for $m_t=20$ and 40 GeV. Here Δ is defined by

$$\Delta=[(\delta m)^2+\tfrac{1}{4}(\delta\Gamma)^2]/[2\Gamma^2+(\delta m)^2-\tfrac{1}{4}(\delta\Gamma)^2] \qquad (34)$$

with $\delta m=m_S-m_L$, $\delta\Gamma=\Gamma_S-\Gamma_L$, and $\Gamma=\frac{1}{2}(\Gamma_S+\Gamma_L)$. The large mixing effects in these calculations are driven primarily by $\delta m/\Gamma$. Solution I gives the larger mixing, which increases with m_t. For $|b\to c|>0.25$ the mixing is small.

B. LH-singlet model

For $s_2=0$, as we assumed in Sec. IIB, there is no first-order $b\to d$ neutral current. The one-loop order-G_F^2 analysis of δm is altered, because there is no t quark; neglecting the small contributions involving u quarks, there is a direct relation between the B system and the K system,

$$\frac{\delta m^2(B)}{\delta m^2(K)}=\frac{U_{cb}^{\ 2}}{U_{cs}^{\ 2}}=\frac{s_3^{\ 2}}{c_3^{\ 2}}\simeq 0.09^{+0.17}_{-0.09}. \qquad (35)$$

This will give negligible mixing from $\delta m^2/\Gamma^2$, since also $\Gamma(B)\gg\Gamma(K)$.

For s_2 very small but not zero, a neutral-current contribution to δm of order G_F arises, for which $\delta m(B)\gg\delta m(K)$ is possible for certain very small values for s_3. Appreciable B-$\bar{B}$ mixing could in principle arise in this way.

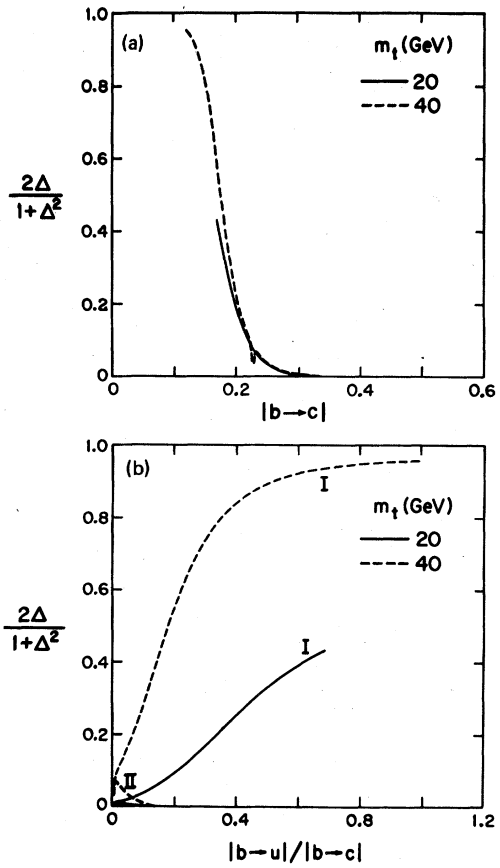

FIG. 14. Standard-model predictions of B^0-$\bar{B}^0$ mixing. Predictions for $2\Delta/(1+\Delta^2)$ from the two solution classes are shown vs $|b\to c|$ and $|b\to u|/|b\to c|$ for various choices of the t-quark mass m_t.

C. RH-doublet model

We consider this model in the limit where $(c,b)_R$ is the only b-changing current. In the one-loop order-G_F^2 calculation of δm^2, with neglect of light quark (u,d,s) contributions, $\delta m(K)$ is given by left-left couplings with c-quark exchange, $\delta m(D)$ is given by left-right couplings with b-quark exchange, and $\delta m(B)$ is given by left-right couplings with c-quark exchange; see Fig. 15. Taking the leading terms[53] we obtain to leading order in the vacuum insertion approximation

$$\begin{aligned}\delta m(K)&=-Kf_K^{\ 2}m_K m_c^{\ 2}U_{cs}^{\ 2}U_{cd}^{\ 2},\\ \delta m(D)&=Kf_D^{\ 2}m_D m_b^{\ 2}U_{bu}^{\ 2}2[\ln(m_W/m_b)-1], \qquad (36)\\ \delta m(B)&=Kf_B^{\ 2}m_B m_c^{\ 2}U_{cd}^{\ 2}2[\ln(m_W/m_c)-1],\end{aligned}$$

where $K=(\alpha G_F)/(6\sqrt{2}\,\pi m_W^{\ 2}x_W)$; f_K, f_D, f_B are the K, D, B decay constants. Compared with stand-

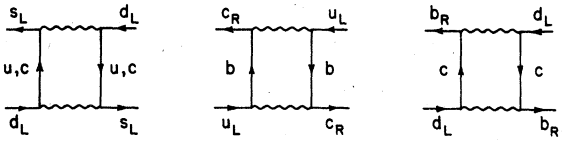

FIG. 15. Effective four-quark interactions contributing to K^0-$\bar{K}^0$, D^0-$\bar{D}^0$, B^0-$\bar{B}^0$ mass differences in the RH-doublet model.

ard-model calculations[51] this $\delta m(D)$ is considerably larger (but still within experimental limits[12,54]) while $\delta m(B)$ is substantially smaller. It is therefore unlikely that large B^0-$\bar{B}^0$ mixing can arise from this mechanism.

With singlet-doublet mixing in either the left- or right-handed sector, the RH-doublet model would admit first-order $\bar{b}d$ neutral currents that could produce large B^0-$\bar{B}^0$ mixing.

ACKNOWLEDGMENTS

We thank W. F. Long for consultations on standard-model results. We are grateful to E. Thorndike, S. H. H. Tye, and M. E. Peskin for stimulating discussions at the CLEO Workshop on B decays. We thank E. Gabathuler for communicating the latest EMC results.

This research was supported in part by the University of Wisconsin Research Committee with funds granted by the Wisconsin Alumni Research Foundation, and in part by the Department of Energy under Contract No. DE-AC0276ER00881-190 and DE-AC0276CH00016.

[1]V. Barger and S. Pakvasa, Phys. Lett. 81B, 195 (1979).
[2]G. Branco and H. P. Nilles, Nucl. Phys. B151, 529 (1979).
[3]G. L. Kane, University of Michigan Report No. UMHE 80-18 (unpublished).
[4]M. Gorn and E. A. Paschos, Phys. Lett. 101B, 255 (1981).
[5]E. H. Thorndike, in *High Energy Physics—1980*, proceedings of XXth International Conference, Madison, Wisconsin, 1980, edited by L. Durand and L. G. Pondrom (AIP, New York, 1981), p. 705; C. Bebek *et al.*, Phys. Rev. Lett. 46, 84 (1981); K. Chadwick *et al.*, *ibid.* 46, 88 (1981).
[6]M. E. Peskin and S.-H. H. Tye, reports to Cornell Workshop on B decays, 1981 (unpublished).
[7]M. Kobayashi and T. Maskawa, Progr. Theor. Phys. 49, 652 (1973). For an early discussion of standard-model phenomenology, see J. Ellis, M. K. Gaillard, D. V. Nanopoulos, and M. Rudaz, Nucl. Phys. B131, 285 (1977).
[8]R. E. Shrock and L. L. Wang, Phys. Rev. Lett. 41, 1692 (1978).
[9]V. Barger, W. F. Long, and S. Pakvasa, Phys. Rev. Lett. 42, 1585 (1979).
[10]R. E. Shrock, S. B. Treiman, and L. L. Wang, Phys. Rev. Lett. 42, 1589 (1979).
[11]S. Pakvasa, S. F. Tuan, and J. J. Sakurai, Phys. Rev. D 23, 2799 (1981).
[12]G. Feldman *et al.*, Phys. Rev. Lett. 38, 1313 (1977); G. Goldhaber *et al.*, Phys. Lett. 69B, 503 (1977).
[13]For a recent analysis, see J. E. Kim, P. Langacker, M. Levine, and H. H. Williams, Rev. Mod. Phys. 53, 211 (1981).
[14]V. Barger, J. Leveille, and P. M. Stevenson, in *High Energy Physics—1980* (Ref. 5), p. 390.
[15]The differences between our LH-singlet branching fractions and those in Ref. 1 are due to an erroneous overall factor $(1-x_W)$ in the neutral-current terms in Eq. (11) of Ref. 1.
[16]V. Barger, W. F. Long, and S. Pakvasa, J. Phys. G 5, L147 (1979).
[17]V. Barger, T. Gottschalk, and R. J. N. Phillips, Phys. Lett. 82B, 445 (1979).
[18]A. Ali, Z. Phys. C 1, 25 (1979).
[19]R. Odorico and V. Roberto, Nucl. Phys. B136, 333 (1978); V. Barger, T. Gottschalk, and R. J. N. Phillips, Phys. Lett. 70B, 51 (1977).
[20]V. Barger, T. Gottschalk, and R. J. N. Phillips, Phys. Rev. D 16, 746 (1977).
[21]For a review see G. Goldhaber and J. E. Wiss, Annu. Rev. Nucl. and Part. Sci. 30, 337 (1980).
[22]M. Suzuki, Phys. Lett. 68B, 164 (1977); J. D. Bjorken, Phys. Rev. D 17, 171 (1978).
[23]R. J. N. Phillips, Nucl. Phys. B153, 475 (1979).
[24]R. M. Barnett, Phys. Rev. D 14, 70 (1976); H. Georgi and H. D. Politzer, Phys. Rev. Lett. 36, 1281 (1976).
[25]J. Babcock and D. Sivers, Phys. Rev. D 18, 2391 (1978); M. A. Shifman, A. I. Vainshtein, and V. I. Zacharov, Nucl. Phys. B136, 157 (1978).
[26]J. P. Leveille and T. Weiler, Nucl. Phys. B147, 147 (1979).
[27]For a review see R. J. N. Phillips, in *High Energy Physics—1980* (Ref. 5), p. 1471.
[28]V. Barger, W. Y. Keung, and R. J. N. Phillips, Phys. Lett. 91B, 253 (1980); T. Weiler, Phys. Rev. Lett. 44, 304 (1980).
[29]S. J. Brodsky, P. Hoyer, C. Peterson, and N. Sakai, Phys. Lett. 93B, 451 (1980).
[30]S. J. Brodsky, C. Peterson, and N. Sakai, Phys. Rev. D 23, 2799 (1981).
[31]A. R. Clark *et al.*, Phys. Rev. Lett. 43, 187 (1979); 45, 682 (1980); 45, 686 (1980).
[32]J. J. Aubert *et al.*, Phys. Lett. 89B, 267 (1980); 94B, 96 (1980); 94B, 101 (1980).
[33]C. Best, Report No. RL-81-044, 1981 (unpublished).
[34]J. F. Owens and E. Reya, Phys. Rev. D 17, 3003 (1978).
[35]M. Holder *et al.*, Phys. Lett. 74B, 277 (1978). A similar bound at lower energy is reported by C. Baltay *et al.*, in *Neutrinos—78*, proceedings of the International Conference for Neutrino Physics and Astrophysics, Purdue, 1978, edited by E. C. Fowler (Purdue

Univ. Press, West Lafayette, Indiana, 1978).
[36]More stringent bounds were claimed by Ref. 30 and by R. J. N. Phillips, Nucl. Phys. B178, 31 (1981), but neither of these works took full account of missing energy and acceptance cuts.
[37]J. G. H. de Groot *et al.*, CERN-Dortmund-Heidelberg-Saclay (CDHS) Collaboration, Phys. Lett. 86B, 103 (1979).
[38]T. Trinko *et al.*, Harvard-Pennsylvania-Wisconsin-Fermilab-Ohio-Rutgers (HPWFOR) Collaboration, Phys. Rev. D 23, 1889 (1981).
[39]K. Nishikawa *et al.*, Caltech-Fermilab-Northwestern-Rochester-Rockefeller (FNRR) Collaboration, Phys. Rev. Lett. 46, 1555 (1981).
[40]H. Goldberg, Phys. Rev. Lett. 39, 1598 (1977); B. L. Young, T. F. Walsh, and T. C. Yang, Phys. Lett. 74B, 111 (1978); V. Barger, T. Gottschalk, and R. J. N. Phillips, Phys. Rev. D 18, 2308 (1978); T. Gottschalk, University of Wisconsin Ph.D. thesis, 1978 (unpublished).
[41]A. Benvenuti *et al.*, Harvard-Pennsylvania-Wisconsin-Fermilab (HPWF) Collaboration, Phys. Rev. Lett. 42, 1024 (1979).
[42]T. Hansl *et al.*, CDHS Collaboration, Nucl. Phys. B142, 381 (1978); J. G. H. de Groot *et al.*, CDHS Collaboration, Phys. Lett. 85B, 131 (1979).
[43]V. Barger, T. Gottschalk, and R. J. N. Phillips, Phys. Rev. D 18, 2308 (1978).
[44]R. Loveless *et al.*, Phys. Lett. 78B, 505 (1978); M. Holder *et al.*, Phys. Lett. 73B, 105 (1978); R. Loveless, in *Proceedings of the Topical Conference on Neutrino Physics at Accelerators*, edited by A. Michette and P. Renton (Rutherford Laboratory, Chilton, Didcot, Oxfordshire, England, 1978).
[45]V. Barger, T. Gottschalk, and R. J. N. Phillips, Phys. Rev. D 19, 92 (1979).
[46]V. Barger, W. Y. Keung, and R. J. N. Phillips, Phys. Lett. 91B, 253 (1980).
[47]V. Barger, W. Y. Keung, and R. J. N. Phillips, Phys. Lett. 92B, 179 (1980).
[48]K. Kleinknecht, report to XVIth Rencontre de Moriond, 1981 (unpublished).
[49]S. Errede, Fermilab seminar, 1981 (unpublished).
[50]A. Ali and Z. Z. Aydin, Nucl. Phys. B148, 165 (1979).
[51]V. Barger, W. F. Long, and S. Pakvasa, Phys. Rev. D 21, 174 (1980).
[52]J. S. Hagelin, Phys. Rev. D 20, 2893 (1979).
[53]M. K. Gaillard, B. W. Lee, and J. L. Rosner, Rev. Mod. Phys. 47, 277 (1975).
[54]V. Barger and E. Ma, J. Phys. G 6, L99 (1980).